Nanoscale

Accepted Manuscript

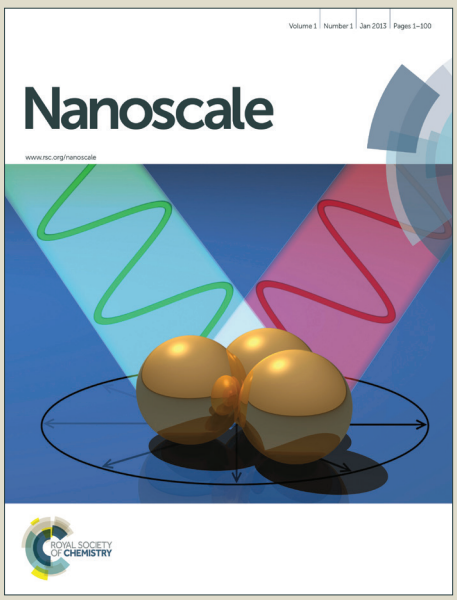

ROYAL SOCIETY OF CHEMISTRY

www.rsc.org/nanoscale

Journal Name

COMMUNICATION

Monitoring Patterned Enzymatic Polymerization on DNA Origami at Single-molecule level

Received 00th January 20xx,
Accepted 00th January 20xx

DOI: 10.1039/x0xx00000x

www.rsc.org/

A. H. Okholm,‡[a] H. Aslan,‡[b] F. Besenbacher,[b] M. Dong*[b] and J. Kjems*[a]

DNA origami has been used to orchestrate reactions with nano-precision using a variety of biomolecules. Here, the dynamics of albumin-assisted, localized single-molecule DNA polymerization by terminal deoxynucleotidyl transferase on a 2D DNA origami are monitored using AFM in liquid. Direct visualization of the surface activity revealed the mechanics of growth.

Spatial control of biomolecular reactions on surfaces is of increasing interest to the emerging field of bionanofabrication. Various biomolecules including DNA[1], RNA[2] and protein[3] have been employed to facilitate spatially arranged reactions at solid-liquid interfaces. However, controlling the position of surface-initiated reactions with molecular resolution remains a great challenge. Since the development of programmable DNA nanostructures and particularly DNA origami[4], DNA has been the favored choice for templating single molecule surface reactions such as strand displacement[5], click chemistry[6] and enzymatic reactions[7]. DNA modifying enzymes are of special interest as they can catalyze a wide range of different surface reactions including, but not limited to, polymerization, hydrolysis and ligation.[8] By taking advantage of the full addressability of DNA origami, researchers have utilized 2D DNA origami templates to study the behavior of different DNA modifying enzymes at surfaces. Using a frame-like DNA origami and fast-scanning AFM, Sugiyama and co-workers have *in situ* visualized the actions of a DNA methyltransferase[9], DNA repair enzymes[10] and a DNA recombinase[11]. A similar approach was used by Subramani et al. to identify a novel DNA binding site in human topoisomerase I.[12]

Another DNA modifying enzyme, the DNA polymerase terminal deoxynucleotidyl transferase (TdT), is naturally found in prelymphocytes, where it facilitates somatic recombination by adding deoxyribonucleotide triphosphates (dNTPs) in a templ[ate]-independent manner to accessible 3' hydroxyl groups. Chilkoti and co-workers used TdT to grow square DNA patches on a gold surface with lateral dimensions down to 100 nm[13,14] and recently more complex DNA micropatterns have been produced in combinatio[n] with irradiation-promoted exchange reaction (IPER)[15]. The resulting DNA brushes have been studied in detail by AFM in air[13], surface plasmon resonance (SPR)[16], X-ray photoelectron spectroscopy (XPS) and near-edge X-ray absorption fine structure (NEXAFS)[17]. TdT [has] recently been used for surface-initiated enzymatic polymerizatio[n] (SIEP)[18] at DNA-patterned interfaces, but never on confined self-assembled DNA nanostructures. To our knowledge, enzymatic activity of TdT has so far not been directly visualized.

TdT is known to be substrate promiscuous. The enzyme accepts many nucleotide analogues at the ribose[19,20], the triphosphate [and] and the nucleobase[22,23], and can, in this way, be used for end-labelling of DNA with a variety of chemical groups. This ability has primed the utilization of TdT in the analysis of DNA fragmentation in cells[24] and for construction of SIEP biosensors[25,26]. We have previously reported the use of TdT to tail DNA oligos with modified nucleotides for functionalization of DNA origami nanostructures with small molecules[27] (biotin, digoxigenin, fluorophores) and macromolecules[23] (dendrimers, polymers and proteins).

Here, we investigated the activity of TdT on a 70×100 nm DNA origami substrate in liquid and found that TdT selectively elongated single stranded protrusions on DNA origami canvases embedded in a surface covered with the protein bovine serum albumin (BSA). We employed liquid tapping mode AFM to visualize single enzymes and monitor the polymerization reaction while exchanging materials in the solution.

To visualize individual enzymes by AFM we prepared DNA canvases containing three staple strands with protruding 3' overhangs of 12 nt at equidistant linear positions, ~24 nm apart (Figure 1a). To minimize side stacking of the DNA canvases, staple strands at the long edges were designed to have single stranded 4 nt loops with the sequence TTTT. Canvases were adsorbed onto the mica; Tris and dTTP (deoxythymidine triphophate) were added while imaging. Immediately after TdT/dTTP addition, enzymes were observed o[n]

[a] Department of Molecular Biology and Genetics, Aarhus University, C. F. Møllers Allé 3, 8000 Aarhus C, Denmark. Center for DNA Nanotechnology and Interdisciplinary Nanoscience Center, Aarhus University, Gustav Wieds Vej 14, 8000 Aarhus C, Denmark.
[b] Center for DNA Nanotechnology and Interdisciplinary Nanoscience Center, Aarhus University, Gustav Wieds Vej 14, 8000 Aarhus C, Denmark.
* Correspondence should be addressed to M.D. (dong@inano.au.dk) or J.K. (jk@mb.au.dk).
‡ These authors contributed equally.
Electronic Supplementary Information (ESI) available. See
DOI: 10.1039/x0xx00000x

the mica and at the positions of protruding single strands as well as at the long edges of the DNA canvases (Figure 1b). We attribute the latter to binding of enzymes to free single stranded T loops by the edges of the origami designed to prevent stacking. Interestingly, no other unspecific binding of the enzyme to the DNA origami was observed. Sequential imaging of DNA canvases over 1 h revealed transient binding of the enzyme to the protruding strands with 1.0 TdT per origami on average (n=111). Even though enzymes were observed to associate and disassociate the total number of enzymes at binding sites was almost constant during 1 h of scanning. In contrast, the adsorption of TdT to the mica surface was found to increase with time (Figure S1). However, no elongation of protruding DNA strands was observed from the recruited enzymes.

It has previously been reported that enzymatic activity on surfaces is improved by the presence of BSA[28]. We therefore investigated the possibility of using BSA to promote nucleotide polymerization. Scanning the surface in the presence of BSA alone showed that it had no affinity to bind the DNA but rather covered the mica where it deposited to a height above the DNA canvases producing an inverted topography at the surface (Figure 2a). To better understand the growth mechanism of BSA on the mica and to rule out the possibility of tip artifacts we injected BSA in the liquid cell whilst scanning the DNA canvases. The height of the DNA canvases, before BSA injection, was measured to be ~2 nm by average line profiling. After the injection, BSA started to cover the mica surface causing the DNA canvases to lose contrast. Within 12 minutes, the BSA grew taller than the DNA canvases by ~8±1.4 nm forming a multilayer surface coating. In conclusion, the BSA mask grew ~10 nm in total (Figure S2). Upon injection of TdT and dTTP to the DNA/BSA system, we consistently observed a vertical growth of up to 3 dots from the structures in less than a minute (Figure 2b). We interpret this as the elongation of the three protruding staple strands by single TdT on each binding site. However, three distinct growing dots were only resolved on a few DNA canvases, while for most canvases the growing regions could not be resolved. We believe this is due to the flexible nature of the elongated single stranded DNA oligos.

To show that the elongation of DNA oligos were specific only to protruding strands, we designed a new pattern on the canvas in the form of the letter A involving approximately half of the 220 staple strands. Staple strands forming the base for letter A were elongated using TdT. TdT was then thermally deactivated prior to DNA origami annealing in order to avoid carry-over of active enzymes to the liquid cell of the AFM. In this way, we were able to control the introduction of enzymes to the sample. Elongation of staple strands was confirmed by gel electrophoresis (Figure S3).

As for the three-dotted design, no polymerization was observed on the newly designed canvases in the absence of BSA (Figure S4). However, when TdT and dTTP were added to the DNA/BSA system, A's clearly formed by vertical growth (Figure 3a). The average speed of growth was determined to be ~1 nm/min based on individual AFM images (The growth was monitored on single images owing to the AFM raster scanning) and after approximately 20 min, the A's had grown to ~20 nm and could not be resolved by the AFM anymore (Figure S5a). When the reaction solution was saturated with dTTP and incubated for 1 h, the growth continued beyond 50 nm (Figure S5b). Formation of A's was observed on approximately half of the DNA canvases, whereas the other half was left unmodified, presumably due to the protruding 3'ends facing down, making them inaccessible to the enzyme (yellow frame in Fig. 3a). In addition to A's we have demonstrated specific TdT activity on other patterns (Figure S6).

To show that the volume expansion was caused by the specific oligonucleotide polymerization mediated by TdT and not for instance protein aggregation, we performed the experiment in absence of protruding staple strands, Co^{2+} or dTTP, all crucial components for the polymerization reaction (Figure S7). None of these conditions gave rise to growth on the DNA canvases. Furthermore, replacement of dTTP with ddUTP, which terminates elongation by capping the 3'end, resulted in the formation of A's that were just visible but unable to grow (Figure 3b). Based on these results we conclude that polymerization of oligodeoxynucleotides by TdT activity is responsible for the observed growth from the DNA canvases.

Considering the ability of TdT to accept nucleotides that have been conjugated to large chemical groups at the nucleobase[23], TdT may be used to functionalize selected oligos on preassembled DNA canvases. To demonstrate this we employed dUTPs conjugated at the base to biotin, fluorescein or 5 kDa polyethylene glycol (PEG) in the polymerization reaction while performing time-resolved liquid AFM (Figure S8).

In conclusion, we report the ability of TdT to site-selectively elongate DNA single strand protrusions from DNA canvases on solid surfaces. AFM in liquid enable real time visualization of individual enzymes and DNA polymerization. We find that a surface mask of bovine serum albumin is required for efficient surface activity of TdT on the DNA canvases. BSA conveniently covers the solid mica surface and leaves the DNA structures untouched. It is frequently used in blocking solutions to prevent unspecific adsorption of proteins[29] and found in many reaction buffers to improve enzyme stability. It is possible that these are indeed the stimulatory effects of the BSA, which were observed in our study. However, this may not be the only explanation. As reported by Niamsiri et al., BSA can interact with and stabilize growing surface polymers[28]. We are currently investigating whether BSA can also interact with the growing DNA polymers and if this is crucial to the activity of TdT. Considering our observations, we believe that the use of BSA masks may facilitate future studies of enzymatic activity on adsorbed DNA origami structures. This could ultimately be of value for the advancement of structural bionanotechnology. The DNA canvas used here consists of 220 pixels separated ~5 nm apart, enabling the design of arbitrary nanopatterns for selective elongation. Furthermore, using TdT together with chemically modified dNTPs, strings of functional groups can be positioned and grown with single-molecule precision on surfaces. The limitless formational capacity of DNA nanostructures and the growing applications of DNA-modifying enzymes may further promote the development of smart interfaces.

Acknowledgements

The authors thank Rasmus Schøler Sørensen for origami designs and synthesis of the pegylated nucleotide. This work was supported by the Danish National Research Foundation

(DNRF81) and Aarhus University, Graduate School of Science and Technology.

Notes and references

1 F. Ozsolak, A. R. Platt, D. R. Jones, J. G. Reifenberger, L. E. Sass, P. McInerney, J. F. Thompson, J. Bowers, M. Jarosz and P. M. Milos, *Nature*, 2009, **461**, 814–8.

2 S. Seetharaman, M. Zivarts, N. Sudarsan and R. R. Breaker, *Nat. Biotechnol.*, 2001, **19**, 336–41.

3 G. Macbeath and S. L. Schreiber, *Science*, 2000, **289**, 1760–1763.

4 P. W. K. Rothemund, *Nature*, 2006, **440**, 297–302.

5 H. Gu, J. Chao, S.-J. Xiao and N. C. Seeman, *Nature*, 2010, **465**, 202–5.

6 N. V Voigt, T. Tørring, A. Rotaru, M. F. Jacobsen, J. B. Ravnsbaek, R. Subramani, W. Mamdouh, J. Kjems, A. Mokhir, F. Besenbacher and K. V. Gothelf, *Nat. Nanotechnol.*, 2010, **5**, 200–3.

7 O. I. Wilner, Y. Weizmann, R. Gill, O. Lioubashevski, R. Freeman and I. Willner, *Nat. Nanotechnol.*, 2009, **4**, 249–54.

8 S. Keller and A. Marx, *Chem. Soc. Rev.*, 2011, **40**, 5690–7.

9 M. Endo, Y. Katsuda, K. Hidaka and H. Sugiyama, *J. Am. Chem. Soc.*, 2010, **132**, 1592–7.

10 M. Endo, Y. Katsuda, K. Hidaka and H. Sugiyama, *Angew. Chem. Int. Ed. Engl.*, 2010, **49**, 9412–6.

11 Y. Suzuki, M. Endo, Y. Katsuda, K. Ou, K. Hidaka and H. Sugiyama, *J. Am. Chem. Soc.*, 2014, **136**, 211–8.

12 R. Subramani, S. Juul, A. Rotaru, F. F. Andersen, K. V Gothelf, W. Mamdouh, F. Besenbacher, M. Dong and B. R. Knudsen, *ACS Nano*, 2010, **4**, 5969–77.

13 D. C. Chow, W.-K. Lee, S. Zauscher and A. Chilkoti, *J. Am. Chem. Soc.*, 2005, **127**, 14122–3.

14 D. C. Chow and A. Chilkoti, *Langmuir*, 2007, **23**, 11712–7.

15 M. N. Khan, V. Tjong, A. Chilkoti and M. Zharnikov, *Angew. Chem. Int. Ed. Engl.*, 2012, **51**, 10303–6.

16 J. Jung and J. Hyun, *BioChip J.*, 2011, **5**, 304–308.

17 M. N. Khan, V. Tjong, A. Chilkoti and M. Zharnikov, *J. Phys. Chem. B*, 2013, **117**, 9929–38.

18 V. Tjong, L. Tang, S. Zauscher and A. Chilkoti, *Chem. Soc. Rev.*, 2014, **43**, 1612–26.

19 K. Ono, *Biochim. Biophys. Acta*, 1990, **1049**, 15–20.

20 V. V. Sosunov, F. Santamaria, L. S. Victorova, G. Gosselin, P Rayner and A. A. Krayevsky, *Nucleic Acids Res.*, 2000, **28**, 1170–5.

21 A. A. Arzumanov, L. S. Victorova, M. V Jasko, D. S. Yesipov and A. A. Krayevsky, *Nucleic Acids Res.*, 2000, **28**, 1276–81

22 A. Kumar, P. Tchen, F. Roullet and J. Cohen, *Anal. Biochem.*, 1988, **169**, 376–382.

23 R. S. Sørensen, A. H. Okholm, D. Schaffert, A. L. B. Kodal, K V. Gothelf and J. Kjems, *ACS Nano*, 2013, **7**, 8098–104.

24 Y. Gavrieli, *J. Cell Biol.*, 1992, **119**, 493–501.

25 V. Tjong, H. Yu, A. Hucknall, S. Rangarajan and A. Chilkot *Anal. Chem.*, 2011, **83**, 5153–9.

26 Y. Wan, P. Wang, Y. Su, X. Zhu, S. Yang, J. Lu, J. Gao, C. Fan and Q. Huang, *Biosens. Bioelectron.*, 2014, **55**, 231–6.

27 K. Jahn, T. Tørring, N. V. Voigt, R. S. Sørensen, A. L. B. Kodal, E. S. Andersen, K. V. Gothelf and J. Kjems, *Bioconjug. Chem.*, 2011, **22**, 819–23.

28 N. Niamsiri, M. Bergkvist, S. C. Delamarre, N. C. Cady, G. W Coates, C. K. Ober and C. A. Batt, *Colloids Surf. B. Biointerfaces*, 2007, **60**, 68–79.

29 W. Senaratne, L. Andruzzi and C. K. Ober, *Biomacromolecules*, 2005, **6**, 2427–48.

Figures

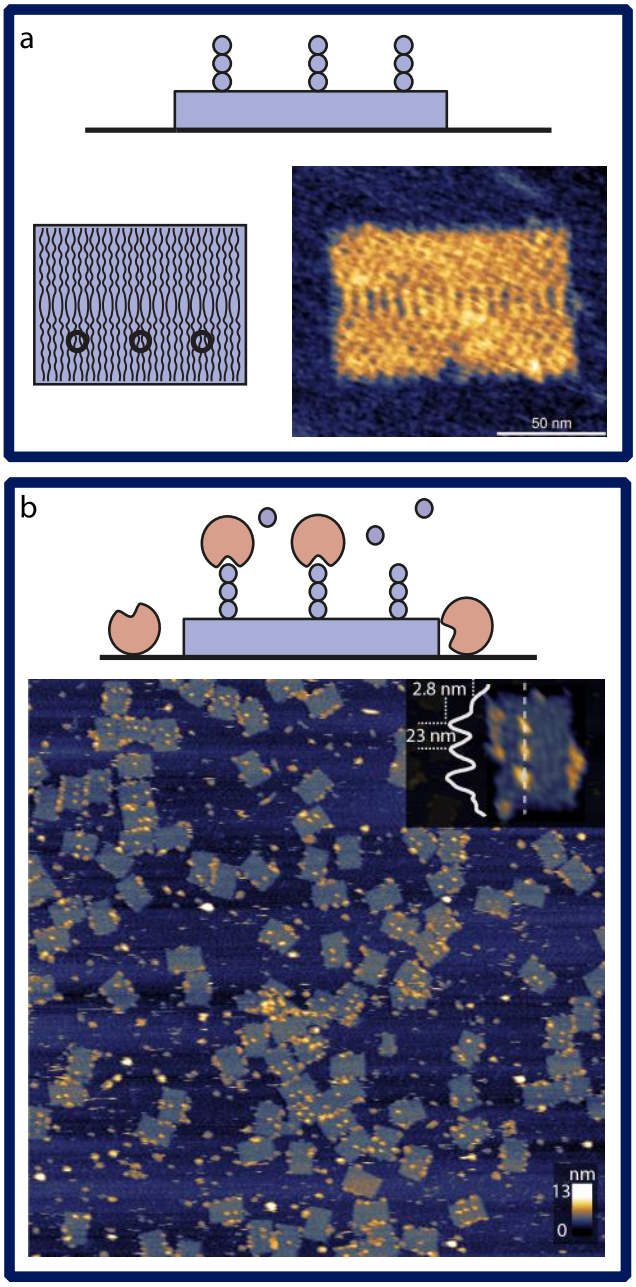

Figure 1. (a) Top: schematic of a DNA canvas in sideview with three staple strands protruding from the 3' end. **Bottom**: topview schematic and liquid AFM image of a DNA canvas. **(b)** Liquid AFM image of DNA canvases incubated with the enzyme TdT (red on schematic) and dTTP. Image size is 2x2 μm. Inset in the AFM image shows a single canvas with TdT bound to the protruding staple strands together with the height profile of the canvas across the dashed line.

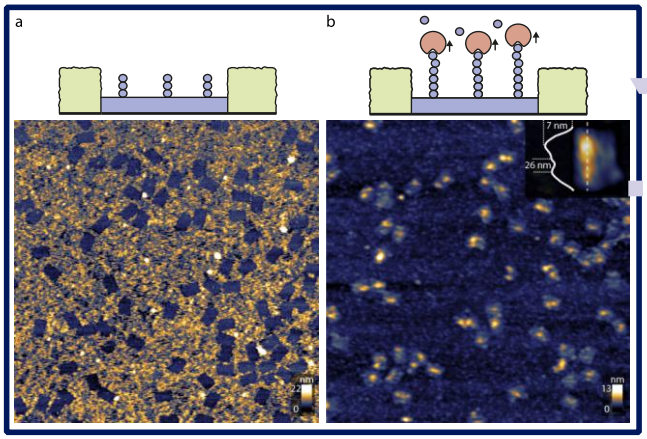

Figure 2. TdT-mediated polymerization on DNA origami in the presence of BSA. Liquid AFM images of DNA canvases containing three protruding staple strands in TdT reaction buffer containing BSA (green on schematics) **(a)** The BSA adsorbed to the mica surface and grew taller than the DNA canvases, reversing the contrast. **(b)** AFM image captured 8 min after injection of TdT and dTTP. Image sizes are 2x2 μm.

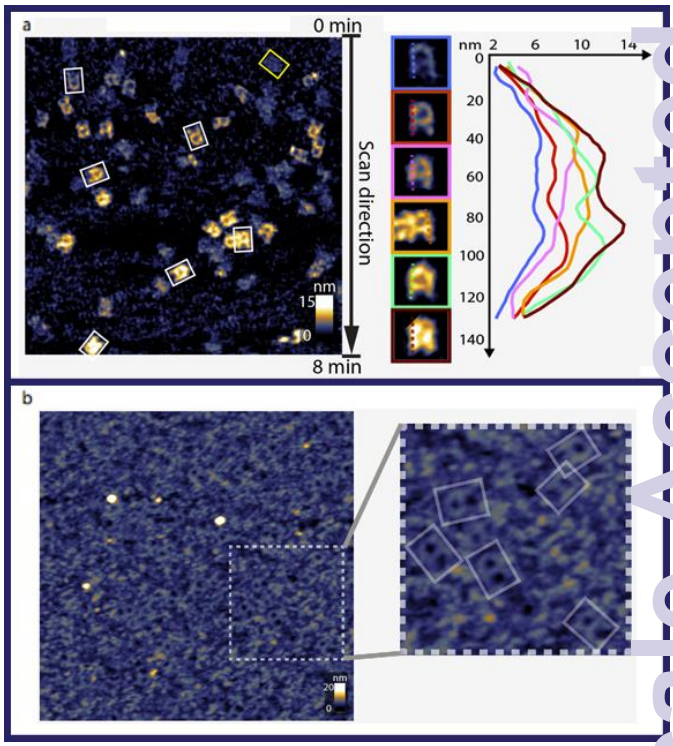

Figure 3. Liquid AFM images of DNA canvases containing protruding staple strands in the pattern of the letter A. **(a) Left:** Single AFM image after injection of TdT and dTTP showing the growth of A's from DNA canvases embedded in BSA. **Right:** Individual canvases framed in the AFM image have been magnified and listed to illustrate the vertical growth. Height profiles (dashed lines on magnified A's) are colored according to frame color **(b)** AFM image after injection of TdT and ddUTP. ddUTP terminates polymerization and no growth was observed. Flat A's formed by stalled enzymes could be observed (white

frames on magnification). Image sizes (except magnified images) are 2x2 μm.